New Journal of Chemistry

Electronic Supplementary Information

The role of hydrogen bonding in tuning CEST contrast efficiency: A comparative study of intra and inter molecular hydrogen bonding

Shalini Pandey, † Subhayan Chakraborty,† Rimilmandrita Ghosh, Divya Radhakrishnan, S. Peruncheralathan* and Arindam Ghosh*

[a] School of Chemical Sciences, National Institute of Science Education and Research ,HBNI, At/PO Jatni, Khurdha 752050 ,Odisha,India

Email: peru@niser.ac.in, aringh@niser.ac.in

Table of Content

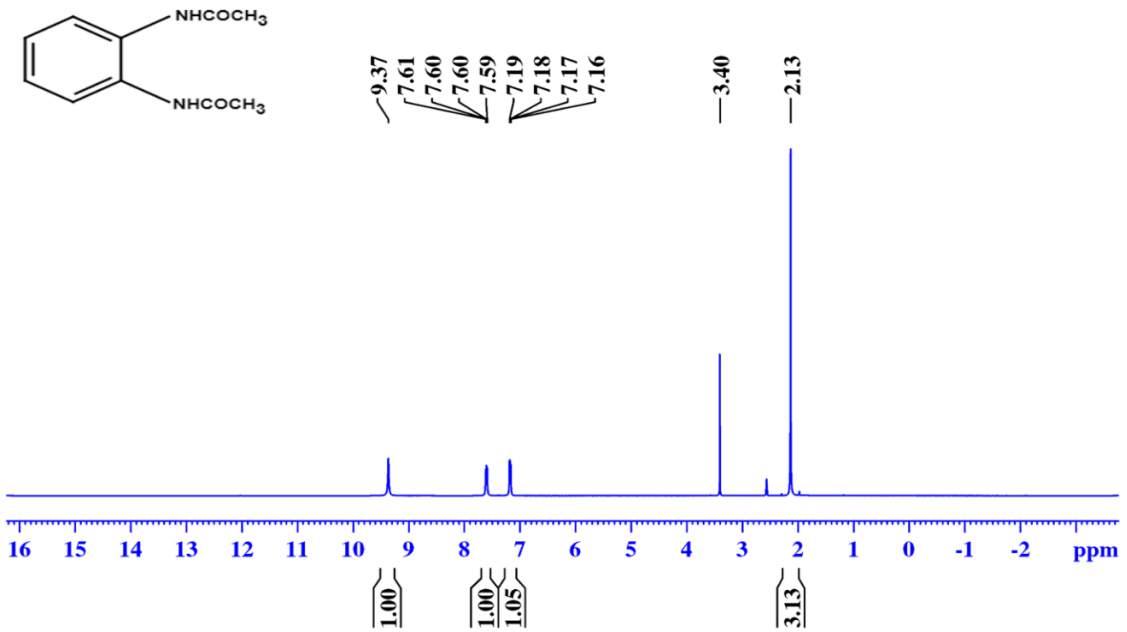

Figure S1.1: ^{1}H-NMR spectrum of *N N'*-(1,2-phenylene)diacetamide (**1**) in DMSO-D_6.

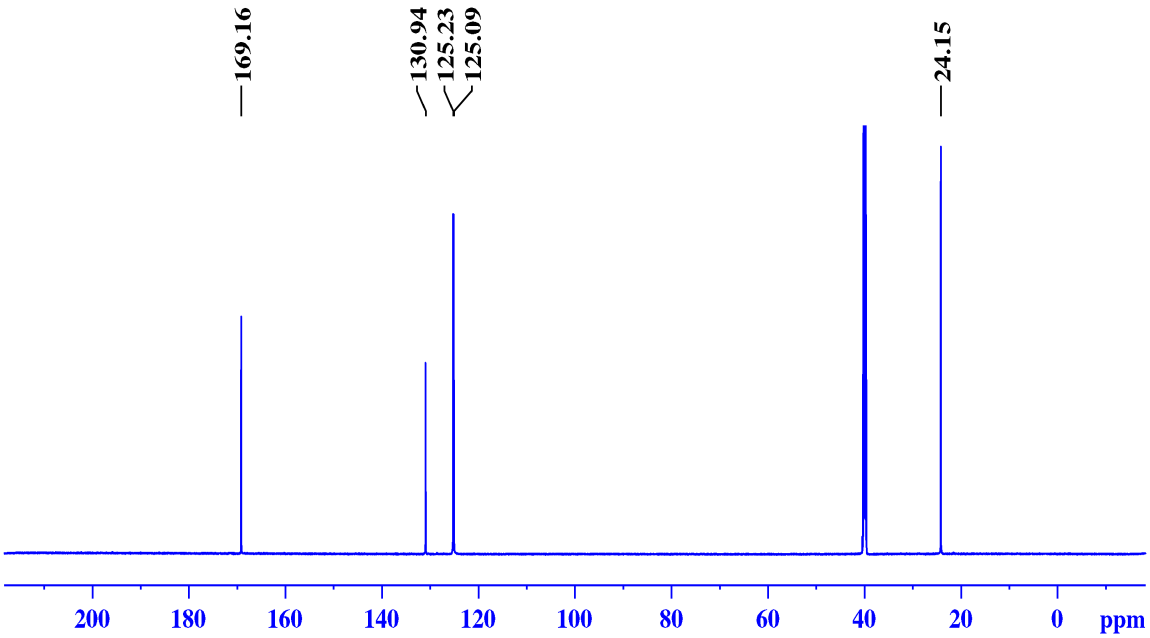

Figure S1.2: ^{13}C NMR spectrum of *N,N'*-(1,2-phenylene)diacetamide (**1**) in DMSO-D_6.

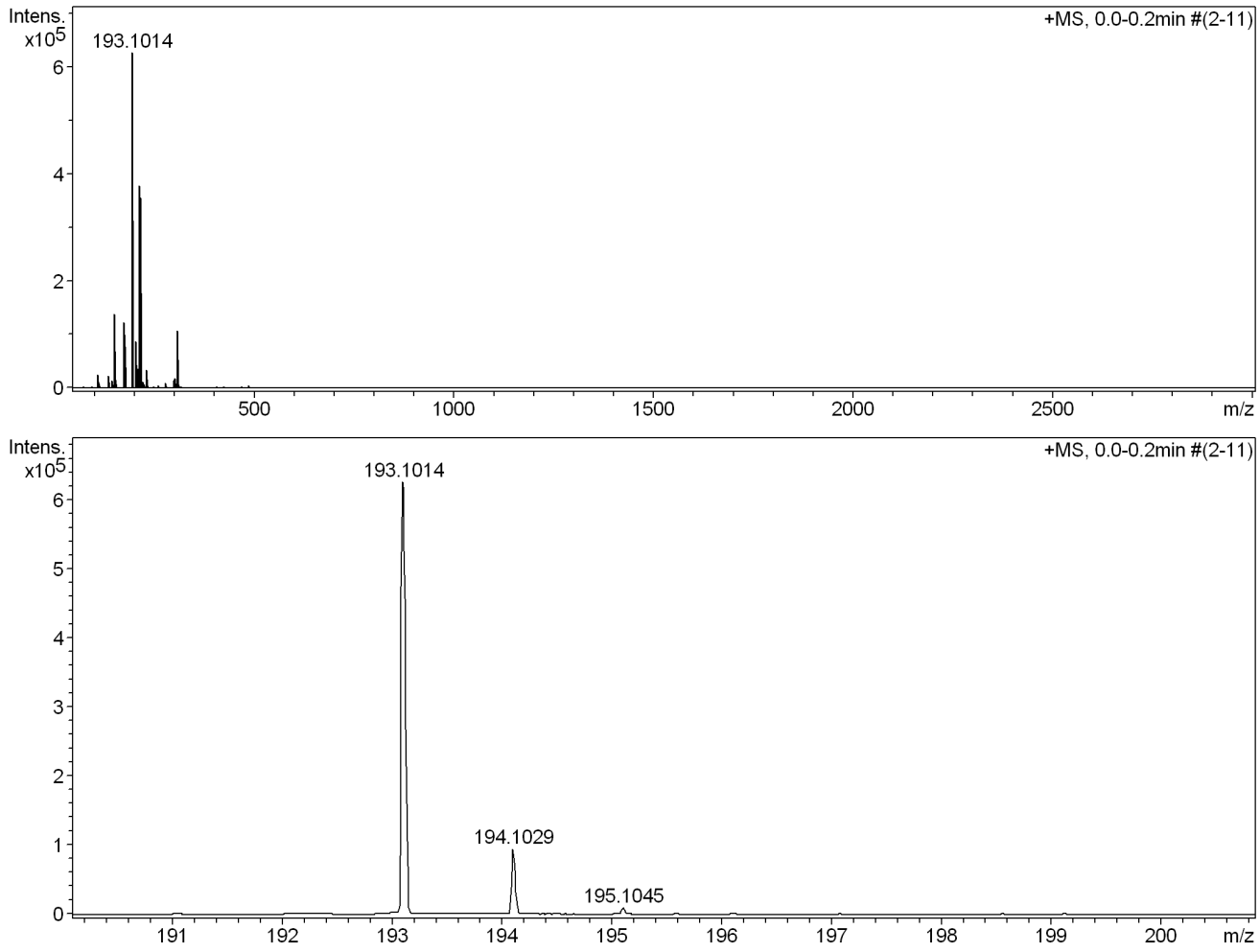

Figure S1.3: Expanded ESI Mass spectra of N,N'-(1,2-Phenylene)diacetamide.

N,N'-(1,2-Phenylene)diacetamide (**1**): ^{1}H NMR (700 MHz, DMSO-d_6) δ 9.37 (s, 1H), 7.61 – 7.58 (m, 1H), 7.18 – 7.16 (m, 1H), 2.13 (s, 3H); ^{13}C NMR (175 MHz, DMSO-d_6) δ 169.1, 130.9, 125.2, 125.0, 24.1. HR-MS (ESI): calculated for $C_{10}H_{12}N_2O_2$ $[M+H]^+$: 193.0972, found, 193.1014.

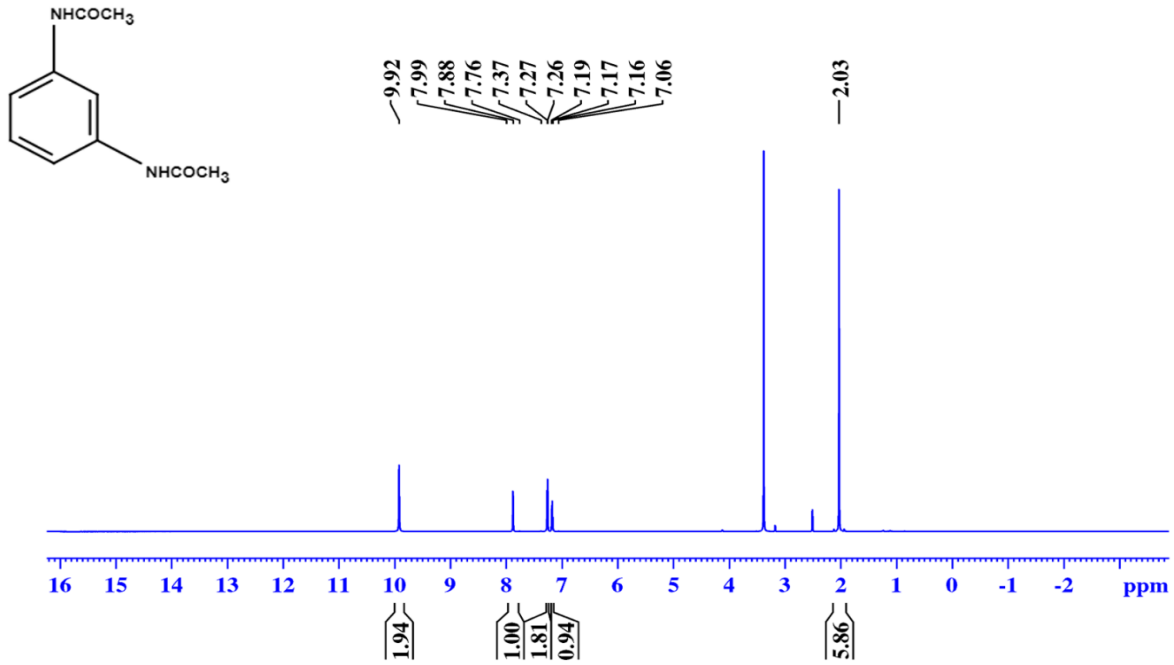

Figure S1.4: ^{1}H-NMR spectrum of *N,N'*-(1,3-phenylene)diacetamide (**2**) in DMSO-D$_6$.

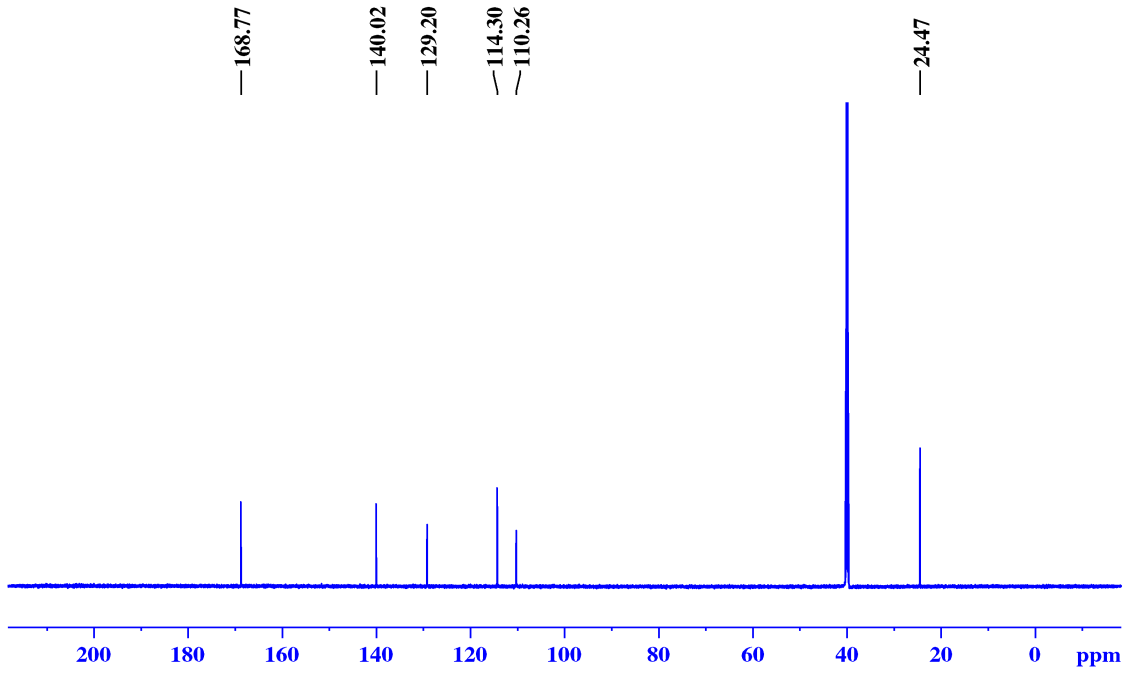

Figure S1.5: ^{13}C NMR spectrum of *N,N'*-(1,3-phenylene)diacetamide (**2**) in DMSO-D$_6$.

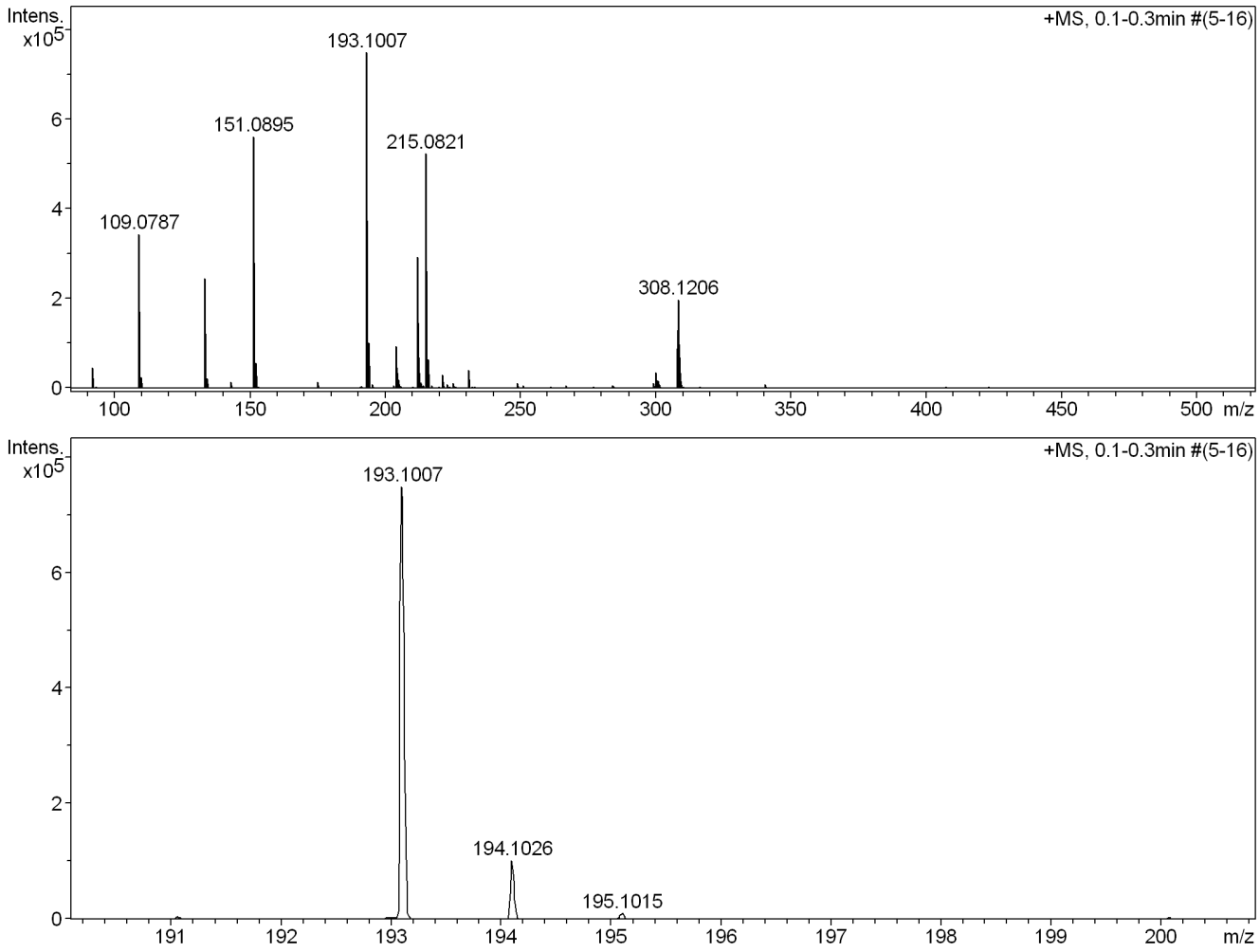

Figure S1.6: Expanded ESI Mass spectra of N,N'-(1,3-Phenylene)diacetamide.

N,N'-(1,3-Phenylene)diacetamide (**2**): ^{1}H NMR (700 MHz, DMSO-d_6) δ 9.92 (s, 1H), 7.88 (s, 1H), 7.26 (d, J = 8.0 Hz, 2H), 7.17 (t, J = 8.0 Hz, 1H), 2.03 (s, 6H); ^{13}C NMR (175 MHz, DMSO-d_6) δ 168.7, 140.0, 129.2, 114.3, 110.2, 24.4. HR-MS (ESI): calculated for $C_{10}H_{12}N_2O_2$ $[M+H]^+$: 193.0972, found, 193.1007.

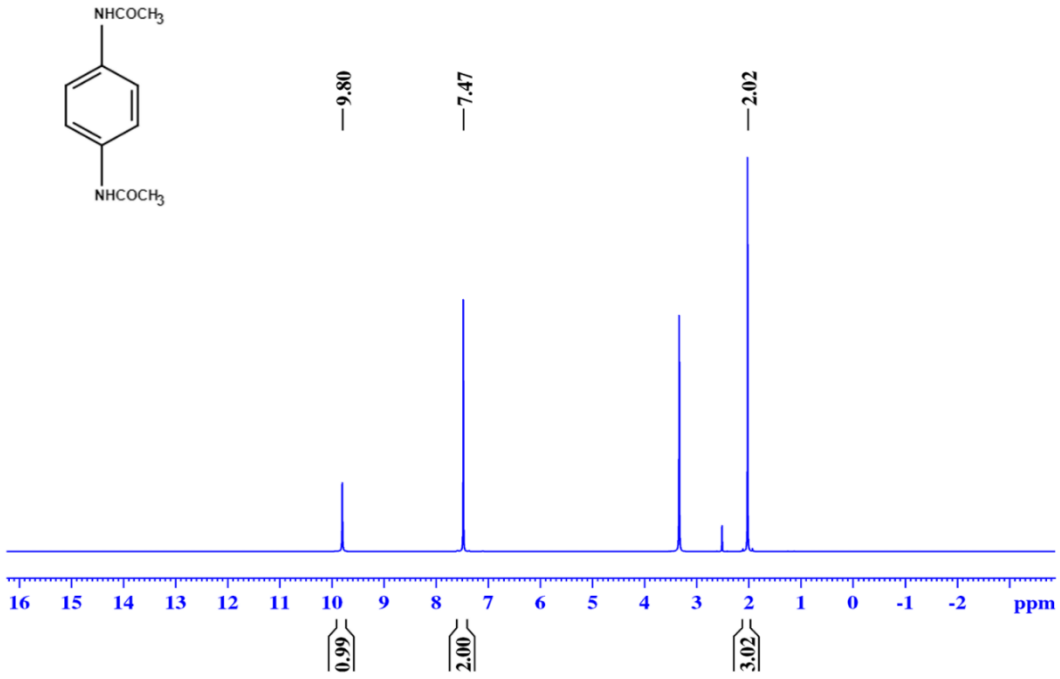

Figure S1.7: ^{1}H NMR spectrum of *N,N'*-(1,4-phenylene)diacetamide (**3**) in DMSO-D_6.

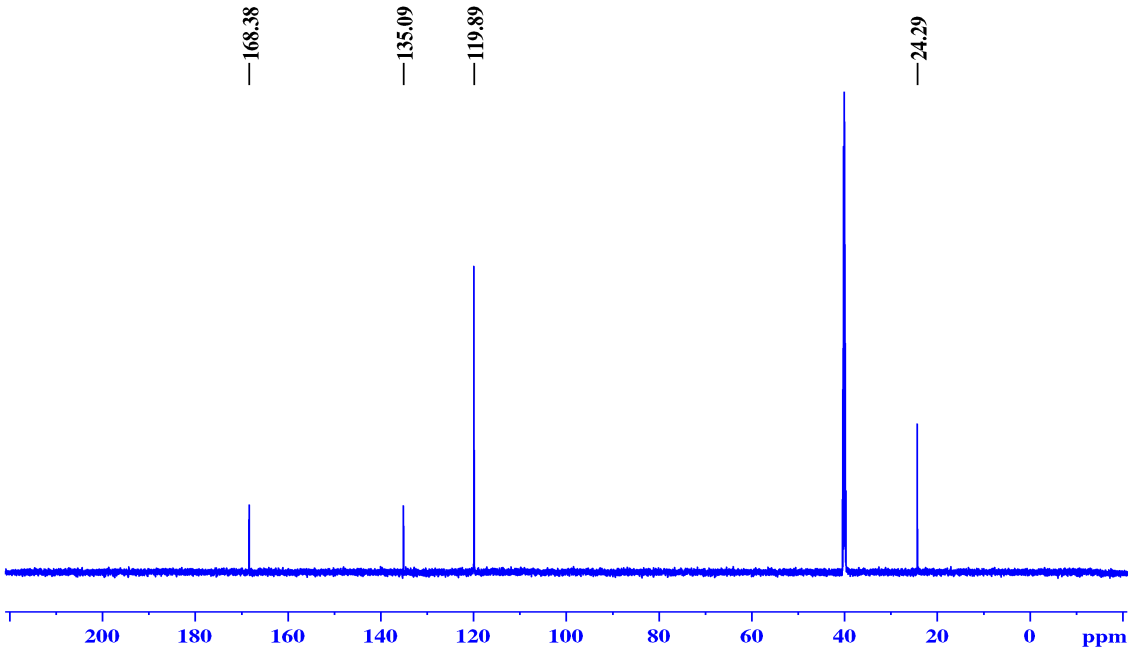

Figure S1.8: ^{13}C NMR spectrum of *N,N'*-(1,4-phenylene)diacetamide (**3**) in DMSO-D_6.

***N,N'*-(1,4-Phenylene)diacetamide** (**3**): ^{1}H NMR (700 MHz, DMSO-d_6) δ 9.79 (s, 1H), 7.47 (s, 2H), 2.01 (s, 3H); ^{13}C NMR (175 MHz, DMSO-d_6) δ 169.3, 135.0, 119.8, 24.2.

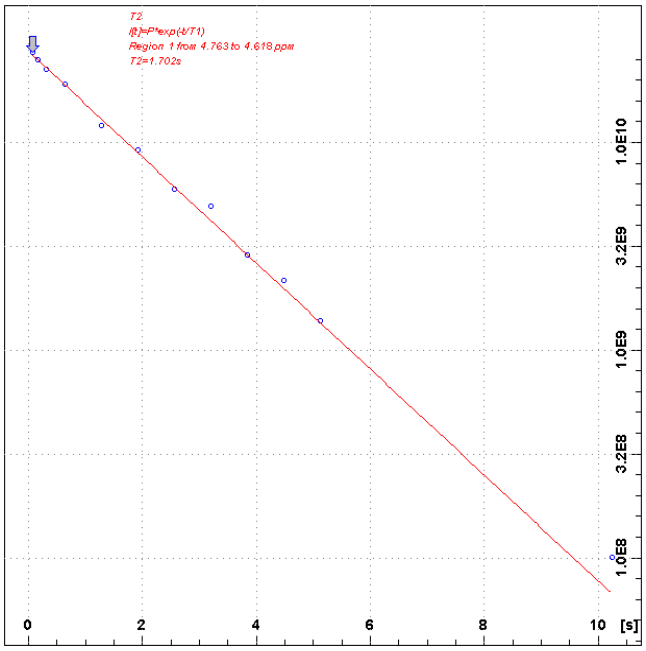

Figure S2.0 : Logarithm of normalized water peak (at 4.7 ppm) intensity as a function of echo delay for determining the transverse relaxation of buffer solution.

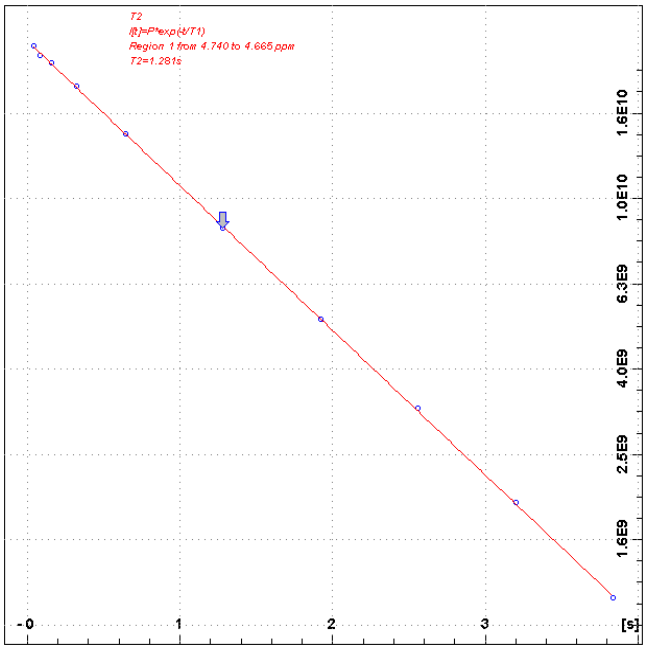

Figure S2.1 : Logarithm of normalized water peak (at 4.7 ppm) intensity as a function of echo delay for determining the transverse relaxation of 15mM solution of **1,** in buffer.

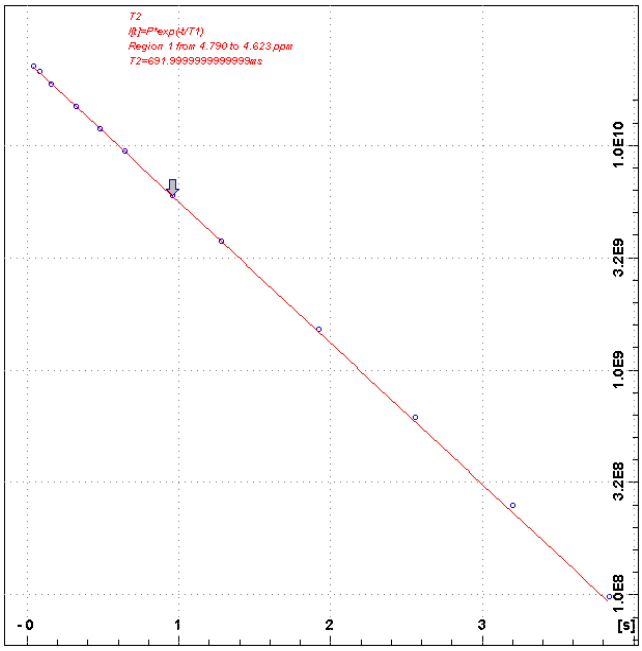

Figure S2.2 : Logarithm of normalized water peak (at 4.7 ppm) intensity as a function of echo delay for determining the transverse relaxation of half diluted saturated solution of **1,** in buffer.

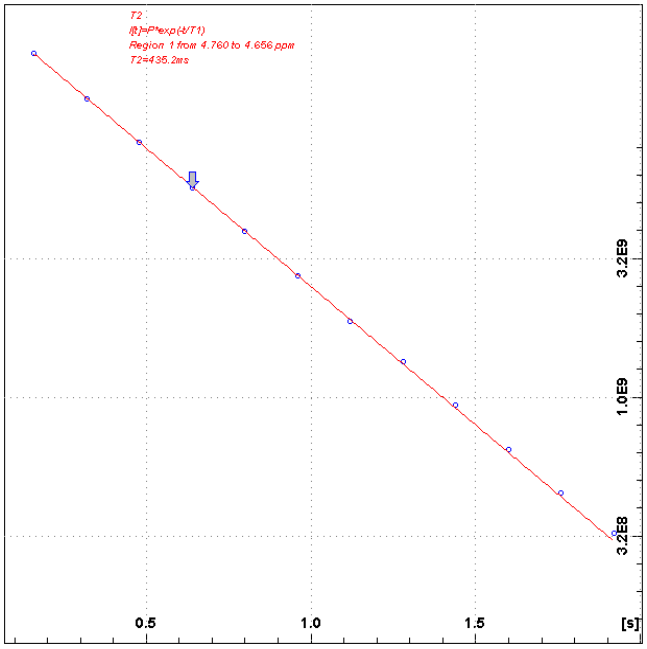

Figure S2.3 : Logarithm of normalized water peak (at 4.7 ppm) intensity as a function of echo delay for determining the transverse relaxation of saturated solution of **1,** in buffer.

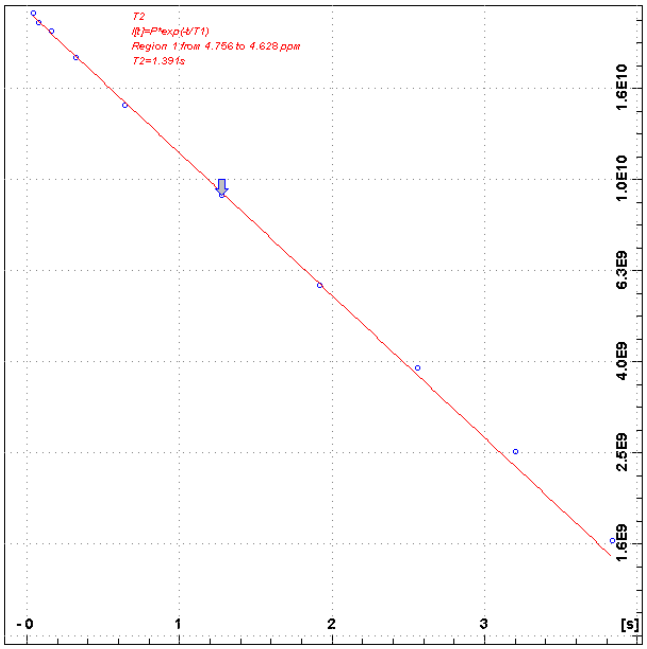

Figure S2.4 : Logarithm of normalized water peak (at 4.7 ppm) intensity as a function of echo delay for determining the transverse relaxation of 15mM solution of **2,** in buffer.

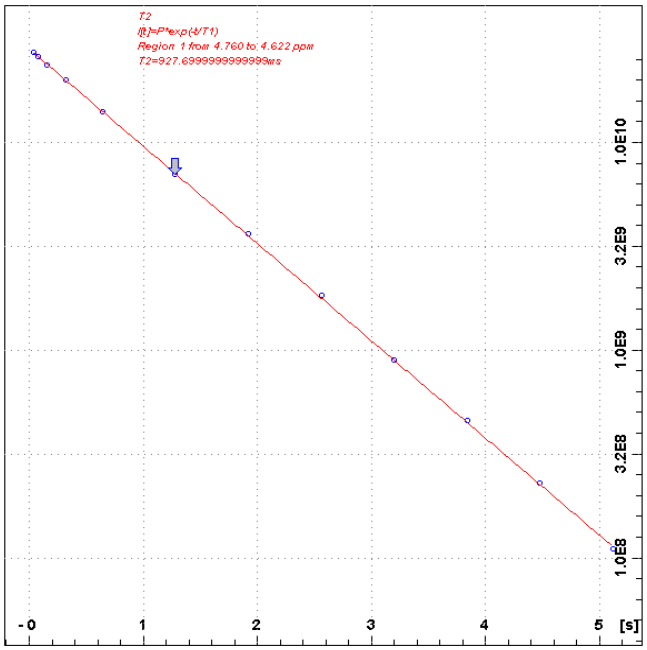

Figure S2.5 : Logarithm of normalized water peak (at 4.7 ppm) intensity as a function of echo delay for determining the transverse relaxation of half diluted saturated solution of **2,** in buffer.

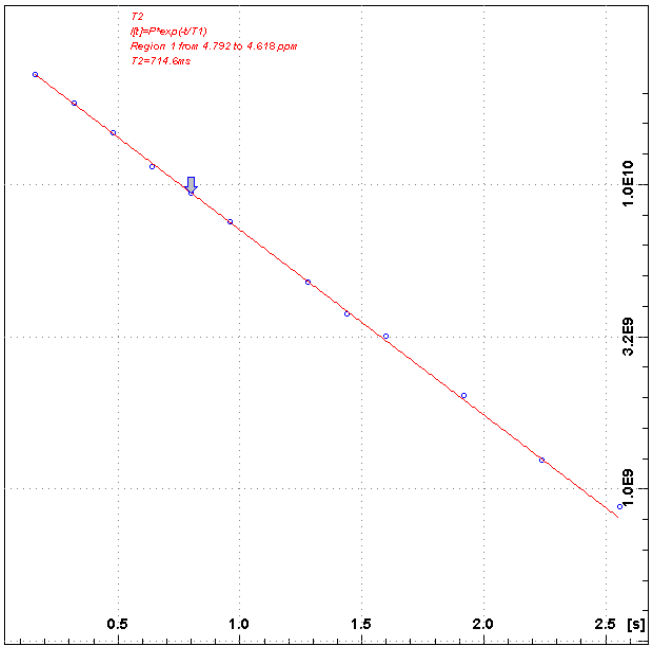

Figure S2.6 : Logarithm of normalized water peak (at 4.7 ppm) intensity as a function of echo delay for determining the transverse relaxation of saturated solution of **2,** in buffer.

a.

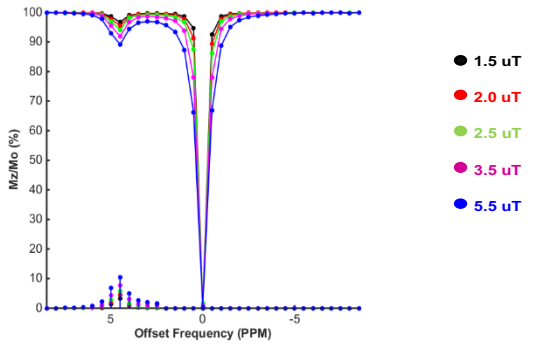

b.

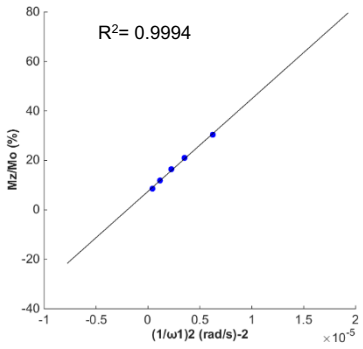

Figure S3: (a) Dependence of CEST percentage on saturation field strength ranging from 1.5 μT to 5.5 μT for *N,N'*-(1,2-phenylene)diacetamide (**1**) at 298K and pH 7.4 (b) Omega plot for exchange rate measurement. The expected linear relationship of $M_z/(M_0-M_z)$ as a function of $1/\omega_1^2$ (rad/sec)$^{-2}$ x 10^{-5} was obtained when recorded at 9.4 T of 15 mM compound in 0.01M PBS buffer at pH 7.4. RF saturation pulse was applied for 6 s ensuring complete saturation

a. b.

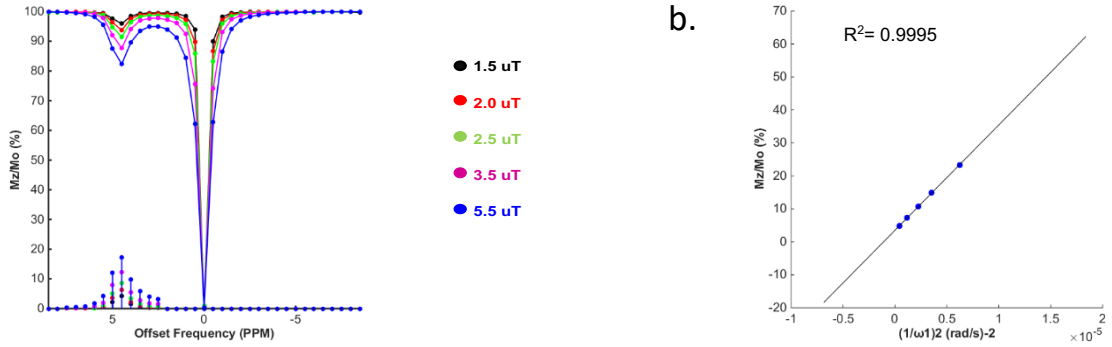

Figure S4: (a) Dependence of CEST percentage on saturation field strength ranging from 1.5 μT to 5.5 μT for *N,N'*-(1,2-phenylene)diacetamide (**1**) at 304K and pH 7.4 (b) Omega plot for exchange rate measurement. The expected linear relationship of $M_z/(M_0-M_z)$ as a function of $1/\omega_1^2$ (rad/sec)$^{-2}$ x 10^{-5} was obtained when recorded at 9.4 T of 15 mM compound in 0.01M PBS buffer at pH 7.4. RF saturation pulse was applied for 6 s ensuring complete saturation.

a. b.

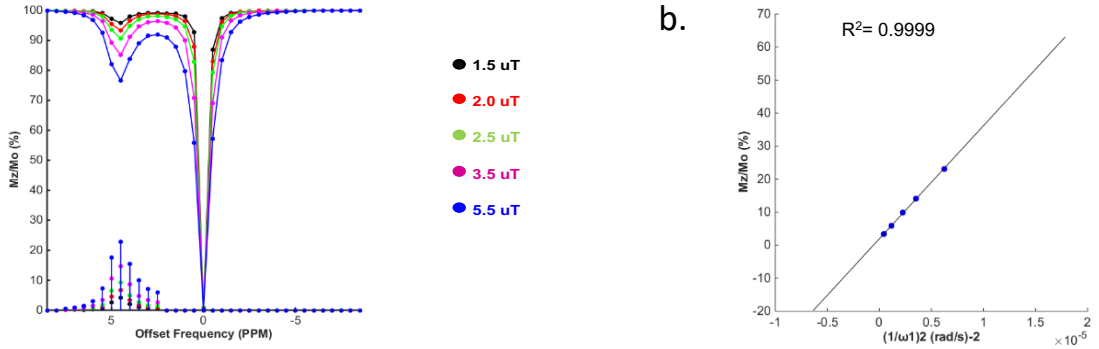

Figure S5: (a) Dependence of CEST percentage on saturation field strength ranging from 1.5 μT to 5.5 μT for *N,N'*-(1,2-phenylene)diacetamide (**1**) at 310K and pH 7.4 (b) Omega plot for exchange rate measurement. The expected linear relationship of $M_z/(M_0-M_z)$ as a function of $1/\omega_1^2$ (rad/sec)$^{-2}$ x 10^{-5} was obtained when recorded at 9.4 T of 15 mM compound in 0.01M PBS buffer at pH 7.4. RF saturation pulse was applied for 6 s ensuring complete saturation.

a. b.

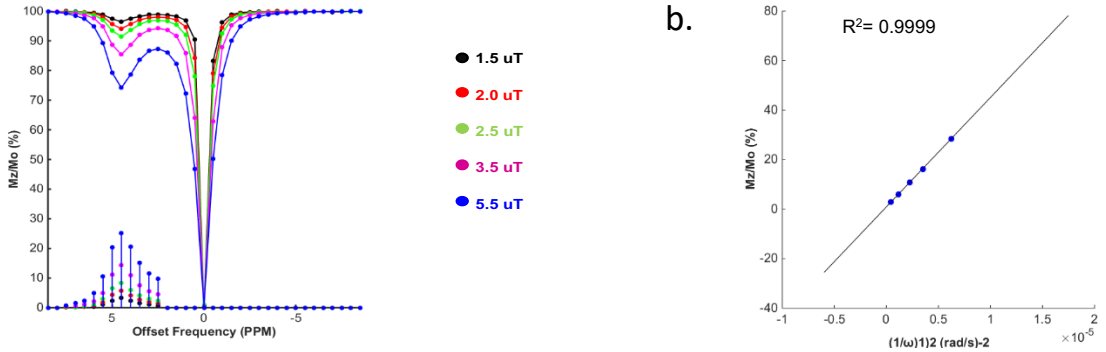

Figure S6: (a) Dependence of CEST percentage on saturation field strength ranging from 1.5 μT to 5.5 μT *N,N'*-(1,2-phenylene)diacetamide (**1**) at 316K (b) Omega plot for exchange rate measurement. The expected linear relationship of $M_z/(M_0-M_z)$ as a function of $1/\omega_1^2$ (rad/sec)$^{-2}$ x 10^{-5} was obtained when recorded at 9.4 T of 15 mM compound in 0.01M PBS buffer at pH 7.4. RF saturation pulse was applied for 6 s ensuring complete saturation.

a.

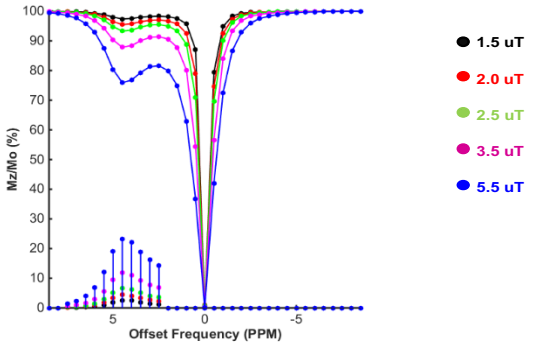

b.

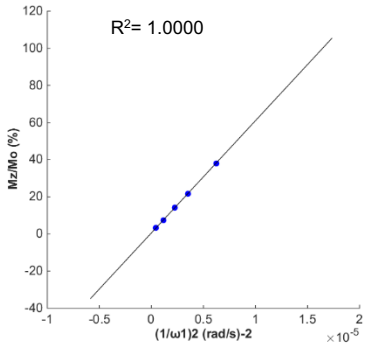

Figure S7: (a) Dependence of CEST percentage on saturation field strength ranging from 1.5 μT to 5.5 μT for *N,N'*-(1,2-phenylene)diacetamide (**1**) at 322K and pH 7.4 (b) Omega plot for exchange rate measurement. The expected linear relationship of $M_z/(M_0-M_z)$ as a function of $1/\omega_1^2$ (rad/sec)$^{-2}$ x 10^{-5} was obtained when recorded at 9.4 T of 15 mM compound in 0.01M PBS buffer at pH 7.4. RF saturation pulse was applied for 6 s ensuring complete saturation.

a.

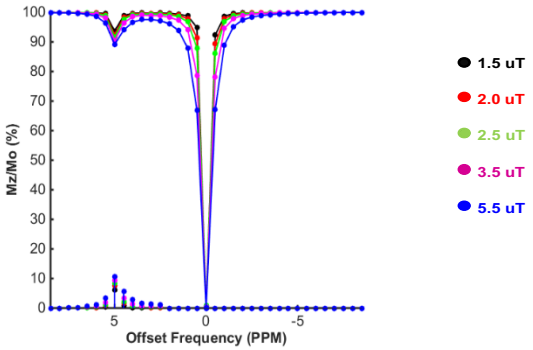

b.

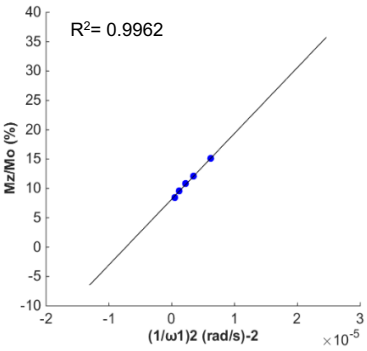

Figure S8: (a) Dependence of CEST percentage on saturation field strength ranging from 1.5 μT to 5.5 μT for *N,N'*-(1,3-phenylene)diacetamide (**2**) at 298K and pH 7.4 (b) Omega plot for exchange rate measurement. The expected linear relationship of $M_z/(M_0-M_z)$ as a function of $1/\omega_1^2$ (rad/sec)$^{-2}$ x 10^{-5} was obtained when recorded at 9.4 T of 15 mM compound in 0.01M PBS buffer at pH 7.4. RF saturation pulse was applied for 6 s ensuring complete saturation.

a.

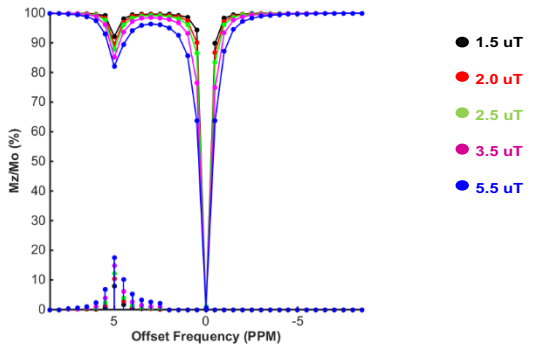

b.

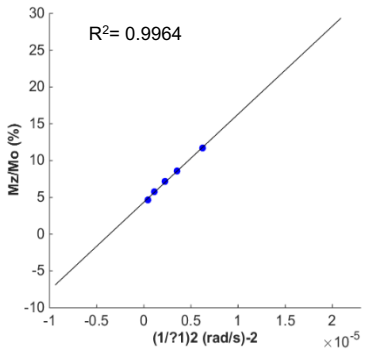

Figure S9: (a) Dependence of CEST percentage on saturation field strength ranging from 1.5 μT to 5.5 μT for *N,N'*-(1,3-phenylene)diacetamide (**2**) at 304K and pH 7.4 (b) Omega plot for exchange rate measurement. The expected linear relationship of $M_z/(M_0-M_z)$ as a function of $1/\omega_1^2$ (rad/sec)$^{-2}$ x 10^{-5} was obtained when recorded at 9.4 T of 15 mM compound in 0.01M PBS buffer at pH 7.4. RF saturation pulse was applied for 6 s ensuring complete saturation.

a. b.

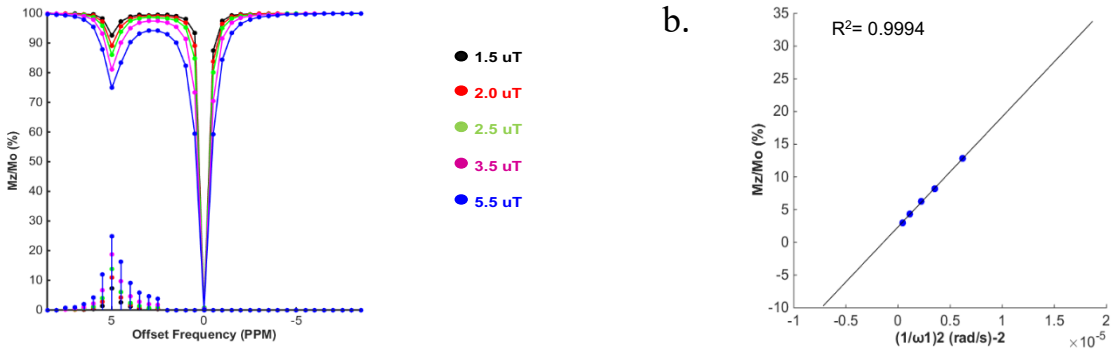

Figure S10: (a) Dependence of CEST percentage on saturation field strength ranging from 1.5 μT to 5.5 μT for *N,N'*-(1,3-phenylene)diacetamide (**2**) at 310K and pH 7.4 (b) Omega plot for exchange rate measurement. The expected linear relationship of $M_z/(M_0-M_z)$ as a function of $1/\omega_1^2$ (rad/sec)$^{-2}$ x 10^{-5} was obtained when recorded at 9.4 T of 15 mM compound in 0.01M PBS buffer at pH 7.4. RF saturation pulse was applied for 6 s ensuring complete saturation.

a. b.

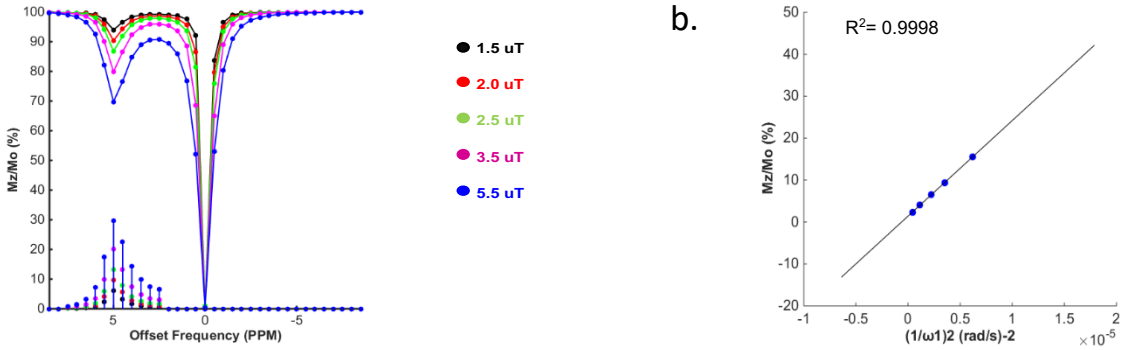

Figure S11: (a) Dependence of CEST percentage on saturation field strength ranging from 1.5 μT to 5.5 μT for *N,N'*-(1,3-phenylene)diacetamide (**2**) at 316K (b) Omega plot for exchange rate measurement. The expected linear relationship of $M_z/(M_0-M_z)$ as a function of $1/\omega_1^2$ (rad/sec)$^{-2}$ x 10^{-5} was obtained when recorded at 9.4 T of 15 mM compound in 0.01M PBS buffer at pH 7.4. RF saturation pulse was applied for 6 s ensuring complete saturation.

a. b.

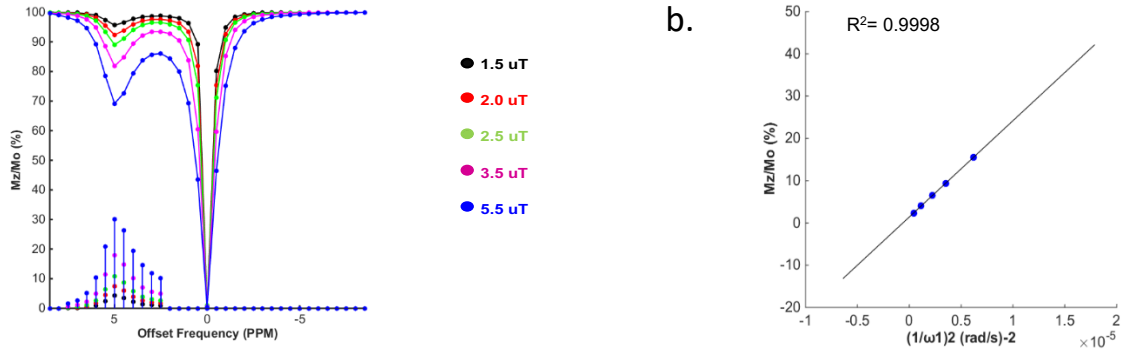

Figure S12: (a) Dependence of CEST percentage on saturation field strength ranging from 1.5 μT to 5.5 μT for *N,N'*-(1,3-phenylene)diacetamide (**2**) at 322K and pH 7.4 (b) Omega plot for exchange rate measurement. The expected linear relationship of $M_z/(M_0-M_z)$ as a function of $1/\omega_1^2$ (rad/sec)$^{-2}$ x 10^{-5} was obtained when recorded at 9.4 T of 15 mM compound in 0.01M PBS buffer at pH 7.4. RF saturation pulse was applied for 6 s ensuring complete saturation.

a.

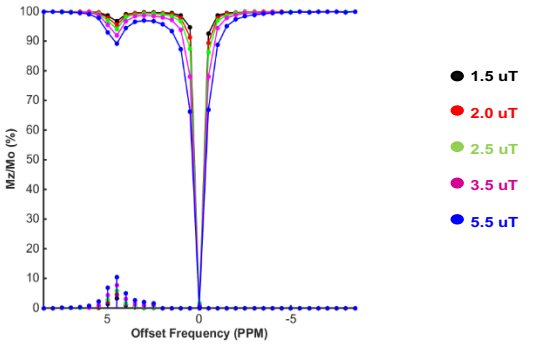

b.

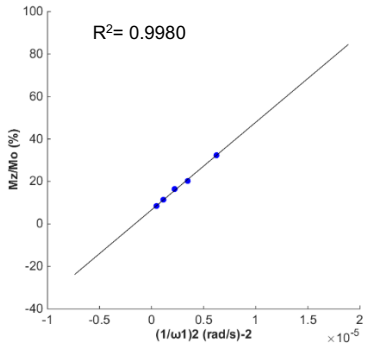

Figure S13: (a) Dependence of CEST percentage on saturation field strength ranging from 1.5 μT to 5.5 μT for *N,N'*-(1,2-phenylene)diacetamide (**1**) at 310K and pH 6.5 (b) Omega plot for exchange rate measurement. The expected linear relationship of $M_z/(M_0-M_z)$ as a function of $1/\omega_1^2$ (rad/sec)$^{-2}$ x 10^{-5} was obtained when recorded at 9.4 T of 15 mM compound in 0.01M PBS buffer at pH 6.5. RF saturation pulse was applied for 6 s ensuring complete saturation.

a.

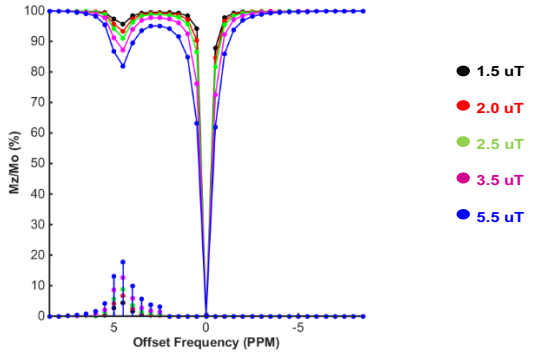

b.

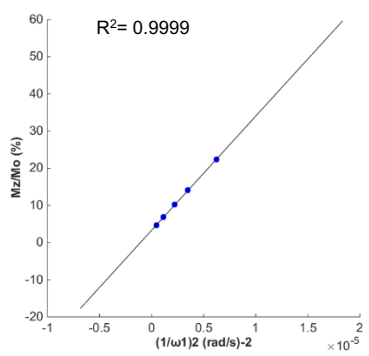

Figure S14: (a) Dependence of CEST percentage on saturation field strength ranging from 1.5 μT to 5.5 μT for *N,N'*-(1,2-phenylene)diacetamide (**1**) at 310K and pH 7.0 (b) Omega plot for exchange rate measurement. The expected linear relationship of $M_z/(M_0-M_z)$ as a function of $1/\omega_1^2$ (rad/sec)$^{-2}$ x 10^{-5} was obtained when recorded at 9.4 T of 15 mM compound in 0.01M PBS buffer at pH 7.0. RF saturation pulse was applied for 6 s ensuring complete saturation.

a.

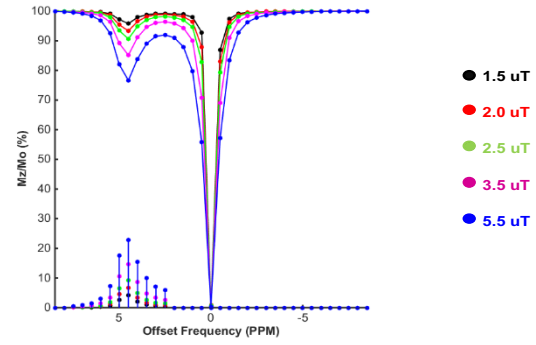

b.

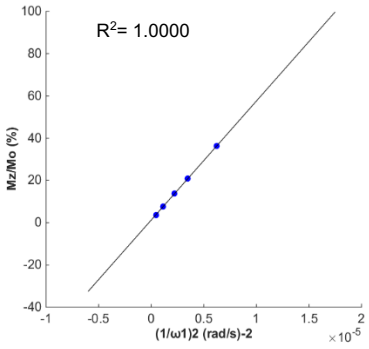

Figure S15: (a) Dependence of CEST percentage on saturation field strength ranging from 1.5 μT to 5.5 μT for *N,N'*-(1,2-phenylene)diacetamide (**1**) at 310K and pH 7.4 (b) Omega plot for exchange rate measurement. The expected linear relationship of $M_z/(M_0-M_z)$ as a function of $1/\omega_1^2$ (rad/sec)$^{-2}$ x 10^{-5} was obtained when recorded at 9.4 T of 15 mM compound in 0.01M PBS buffer at pH 7.4. RF saturation pulse was applied for 6 s ensuring complete saturation.

a.

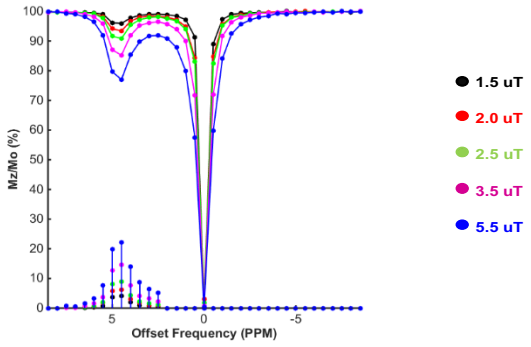

b.

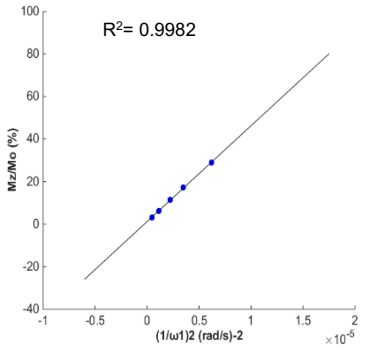

Figure S16: (a) Dependence of CEST percentage on saturation field strength ranging from 1.5 μT to 5.5 μT for *N,N'*-(1,2-phenylene)diacetamide (**1**) at 310K and pH 8.1 (b) Omega plot for exchange rate measurement. The expected linear relationship of $M_z/(M_0-M_z)$ as a function of $1/\omega_1^2$ (rad/sec)$^{-2}$ x 10^{-5} was obtained when recorded at 9.4 T of 15 mM compound in 0.01M PBS buffer at pH 8.1. RF saturation pulse was applied for 6 s ensuring complete saturation.

a.

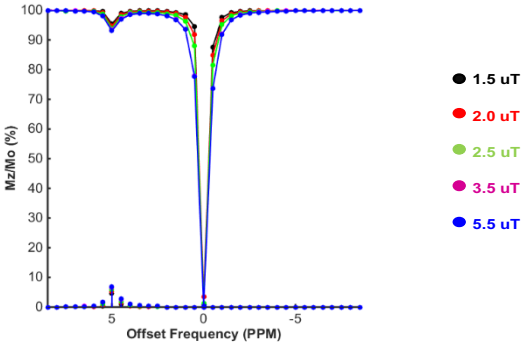

b.

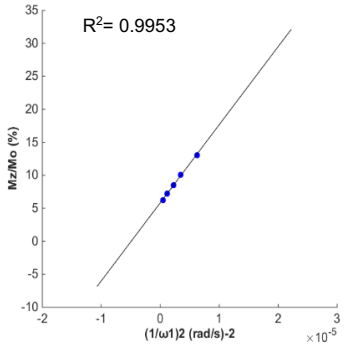

Figure S17: (a) Dependence of CEST percentage on saturation field strength ranging from 1.5 μT to 5.5 μT for *N,N'*-(1,3-phenylene)diacetamide (**2**) at 310K and pH 6.5 (b) Omega plot for exchange rate measurement. The expected linear relationship of $M_z/(M_0-M_z)$ as a function of $1/\omega_1^2$ (rad/sec)$^{-2}$ x 10^{-5} was obtained when recorded at 9.4 T of 15 mM compound in 0.01M PBS buffer at pH 6.5. RF saturation pulse was applied for 6 s ensuring complete saturation.

a.

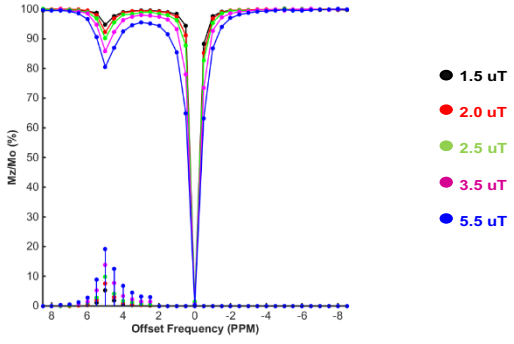

b.

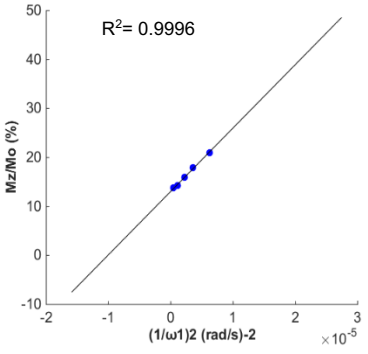

Figure S18: (a) Dependence of CEST percentage on saturation field strength ranging from 1.5 μT to 5.5 μT for *N,N'*-(1,3-phenylene)diacetamide (**2**) at 310K and pH 7.0 (b) Omega plot for exchange rate measurement. The expected linear relationship of $M_z/(M_0-M_z)$ as a function of $1/\omega_1^2$ (rad/sec)$^{-2}$ x 10^{-5} was obtained when recorded at 9.4 T of 15 mM compound in 0.01M PBS buffer at pH 7.0. RF saturation pulse was applied for 6 s ensuring complete saturation.

a.

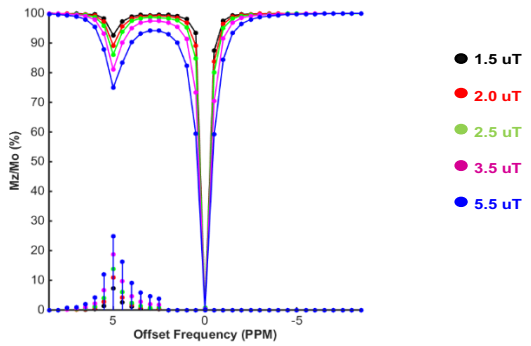

b.

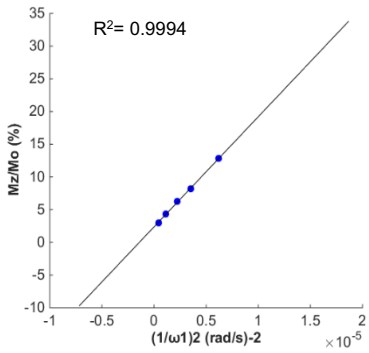

Figure S19: (a) Dependence of CEST percentage on saturation field strength ranging from 1.5 μT to 5.5 μT for *N,N'*-(1,3-phenylene)diacetamide (**2**) at 310K and pH 7.4 (b) Omega plot for exchange rate measurement. The expected linear relationship of $M_z/(M_0-M_z)$ as a function of $1/\omega_1^2$ (rad/sec)$^{-2}$ x 10^{-7} was obtained when recorded at 9.4 T of 15 mM compound in 0.01M PBS buffer at pH 7.4. RF saturation pulse was applied for 6 s ensuring complete saturation.

a.

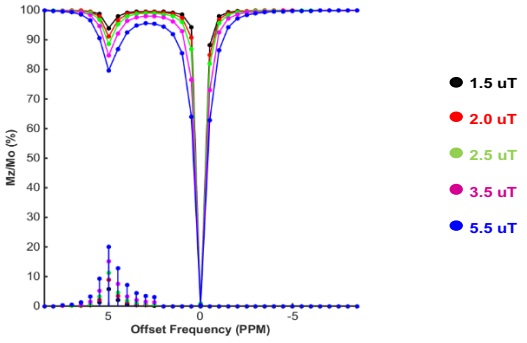

b.

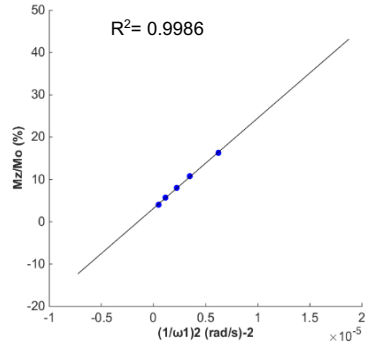

Figure S20: (a) Dependence of CEST percentage on saturation field strength ranging from 1.5 μT to 5.5 μT *N,N'*-(1,3-phenylene)diacetamide (**2**) at 310K and pH 8.1 (b) Omega plot for exchange rate measurement. The expected linear relationship of $M_z/(M_0-M_z)$ as a function of $1/\omega_1^2$ (rad/sec)$^{-2}$ x 10^{-7} was obtained when recorded at 9.4 T of 15 mM compound in 0.01M PBS buffer at pH 8.1. RF saturation pulse was applied for 6 s ensuring complete saturation.

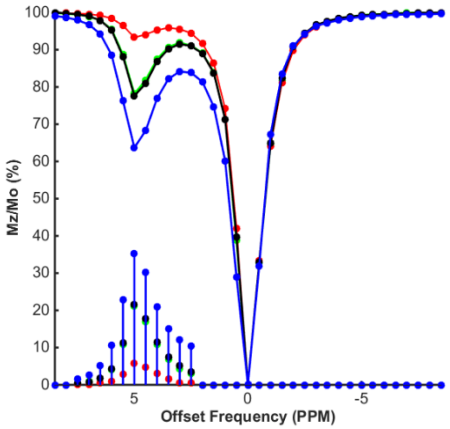

Figure S21: Dependence of CEST effect of *N,N'*-(1,3-phenylene)diacetamide (**2**) on pH. Overlaid Z-spectra with pH ranging from 6.5 to 8.1, RF saturation of 5 μT was applied for 3s to obtain the z-spectra.

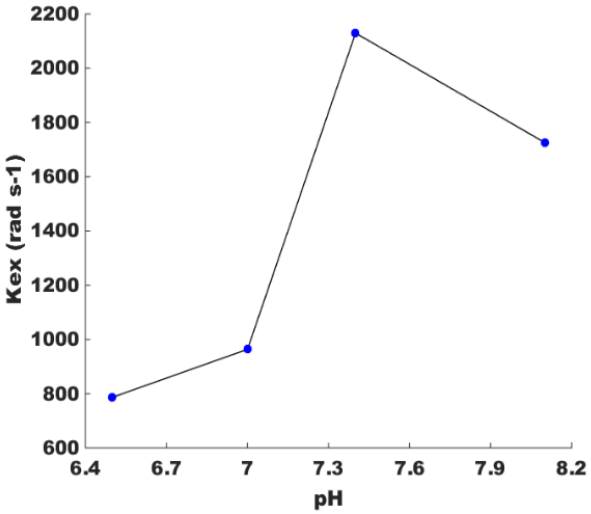

Figure S22: Dependence of k_{ex} for **1**, as a function of pH of buffer solution.

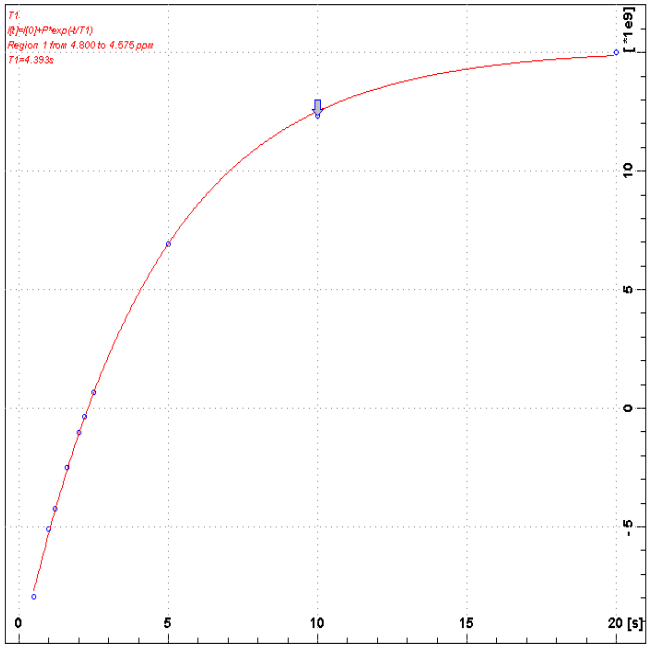

Figure S23.1: Normalized water peak (at 4.7 ppm) intensity as a function of relaxation delay for determining the longitudinal relaxation time constant of water in normal PBS buffer solution.

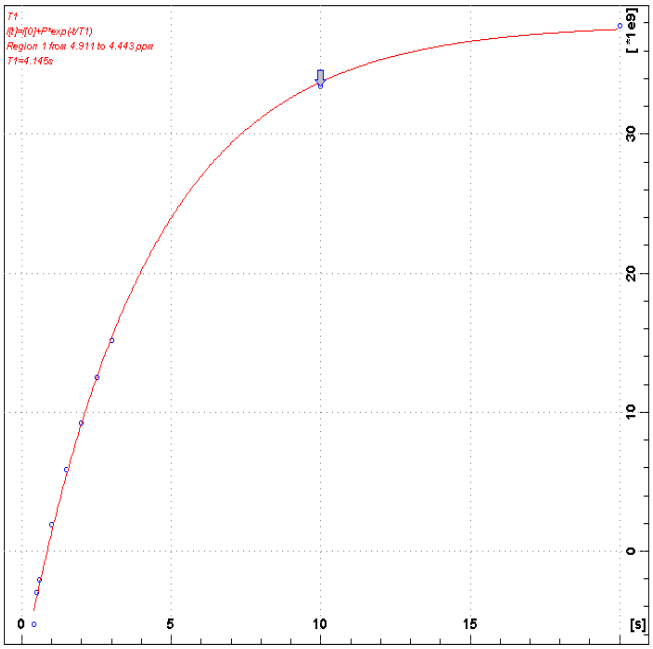

Figure S23.2: Normalized water peak (at 4.7 ppm) intensity as a function of relaxation delay for determining the longitudinal relaxation time constant of water in 15mM solution of **2** in PBS buffer.